

Supplementary Materials
Molecular Biology of the Cell
Janczyk *et al.*

Supplemental Figure Legends

Figure S1. Mad1 accumulates at spindle poles after inhibition of Aurora kinase activity.

A-B) Representative images depicting localization of Mad1 (red) in HeLa T-Rex cells treated with increasing concentrations of Aurora kinases inhibitor VX680, with tubulin (cyan) and centromere (ACA, green) co-staining, bar=5 μm (n = 3). Greyscale images of Mad1 localization are shown in panel B.

C) Quantification of Mad1 fluorescent intensity at the kinetochores (left panel) or at the spindle poles (right panel) in the experiment depicted in panel A (Box, 25–75 percentile; whisker, 5-95 percentile; bar in middle, median. One-way ANOVA, with * $p < 0.05$, *** $p < 0.0005$).

D) Quantification of Mad1 fluorescent intensity at kinetochores (left panel) or at the spindle poles (right panel) relative to ACA fluorescent intensity at kinetochores in the experiment depicted in Figure 1, A-D (Box, 25-75 percentile; whisker, 5-95 percentile, bar in middle, median. One-way ANOVA, with * $p < 0.05$, *** $p < 0.0005$).

E-F) Representative images depicting localization of Mad1 (red) in HeLa T-Rex cells treated with increasing concentrations of Aurora kinases inhibitor AZD1152, with tubulin (cyan) and centromere (ACA, green) co-staining, bar=5 μm (n=3). Greyscale images of Mad1 localization are shown in panel E.

G) Quantification of Mad1 fluorescent intensity at the kinetochores (left panel) or at the spindle poles (right panel) in the experiment depicted in panel C (Box, 25–75 percentile; whisker, 5–95 percentile; bar in middle, median. One-way ANOVA, with n/s $p > 0.05$, *** $p < 0.0005$).

H) Western blot showing the reduction of Aurora B pT232 but not Aurora A pT288 levels upon incubation of HeLa T-Rex cells with increasing concentration of specific Aurora B inhibitor AZD1152

I) Western blot showing the reduction of Aurora A pT288 but not Aurora B pT232 levels upon incubation of HeLa T-Rex cells with increasing concentration of specific Aurora A inhibitor MLN8054.

Figure S2. Novel phosphorylation site Ser285 is localized within predominantly unstructured C-terminal region of Ndel1.

A) Prediction of natively disordered regions of human Ndel1 protein by PrDOS (Ishida and Kinoshida, 2007). Ser285 position is indicated by the black arrow.

B) Coomassie Blue staining of SDS-PAGE gel depicting purified Ndel1 fragments used in experiment shown in Figure 2B.

C) Table representing phosphopeptides detected by LC-MS/MS of Ndel1 8-310 fragment *in vitro* phosphorylated by Aurora B kinase. Blue text indicates S285 site, red S* or T* - detected phosphorylations.

D) pSer285 staining at the poles of *Xenopus laevis* S3 cells disappears in the presence of phosphorylated peptide used to raise the phosphospecific antibody, but not in the presence of unmodified peptide.

E) Representative images depicting the accumulation of Ndel1 signal at spindle poles after treatment with VX680, whereas Ndel1 pS285 signal decreases, bar=5 μ M.

F) Quantification of Ndel1 (upper panel) or Ndel1 pS285 (lower panel) fluorescent intensity (upper panel) at the spindle poles in the experiment depicted in panel B (**p<0.005, ***p< 0.0001, Student's T-test, unpaired).

G) Quantification of Aurora A pT288 fluorescent intensity in three independent DMSO and VX680 treated cells (***p<0.005, Student t-test, unpaired).

Figure S3. Ndel1 phosphorylation regulates cell proliferation and mitotic exit in sensitized background.

A) Western blot showing the efficiency of Ndel1 knockdown and LAP-Ndel1 overexpression in HeLa T-Rex cells

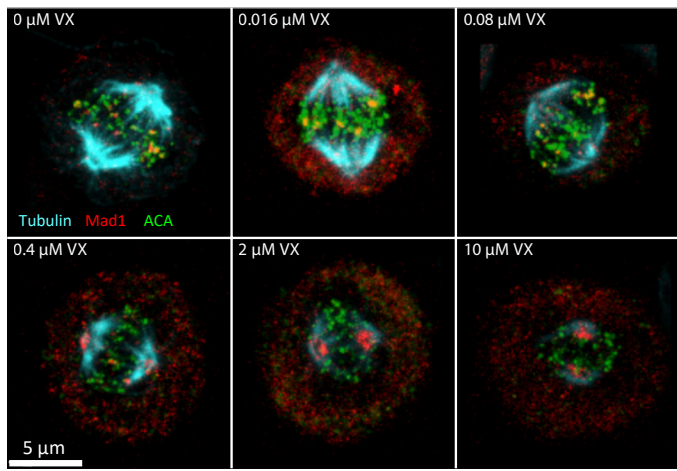
B) A non-phosphorylatable mutant of Ndel1 does not show increased proliferation rates in absence of 20 nM Nocodazole. Graph depicts confluency normalized to day 0 of HeLa T-Rex cells expressing either Ndel1 WT or Ndel1 S285A mutant (n = 3, Student t-test, with n/s – p>0.05).

C-D) Representative brightfield images after background correction and normalization of 5x5 grid of HeLa T-Rex cells expressing Ndel1 WT or Ndel1 S285A grown in presence of 20 nM Nocodazole over prolonged time (C). Masks produced by PHANTAST plugin to ImageJ to visualize measured confluency are shown in (D).

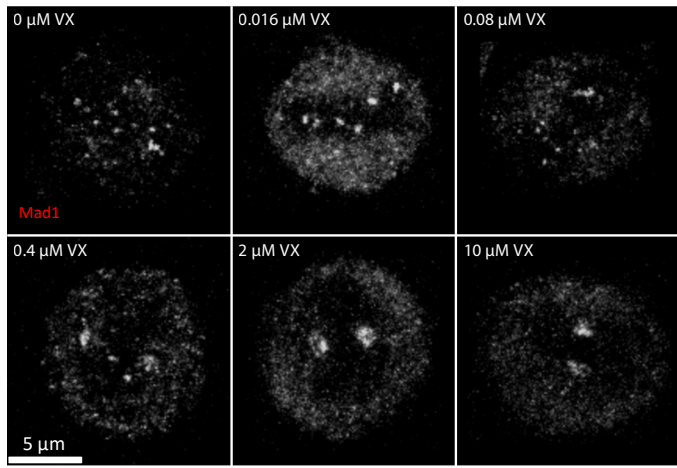
E-F) HeLa T-Rex cells expressing Ndel1 WT or Ndel1 S285A were imaged over 24hrs in presence of 20 nM Nocodazole and 100 nM SiR-DNA dye. Shown are representative images of single cell (white arrow) from NEBD to anaphase (E) or NEBD to mitotic catastrophe (F).

Figure S1

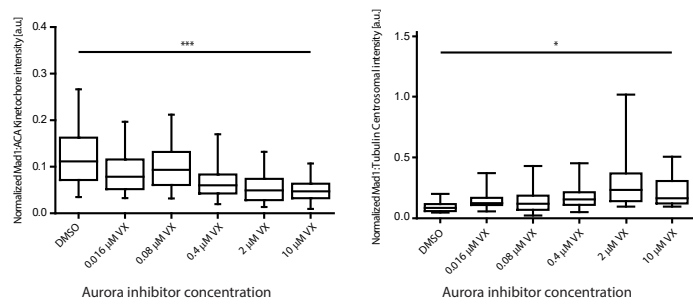
A



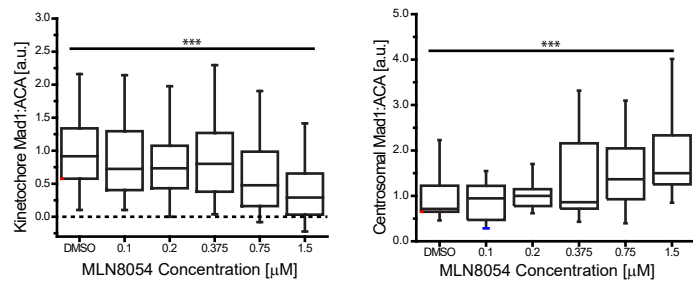
B



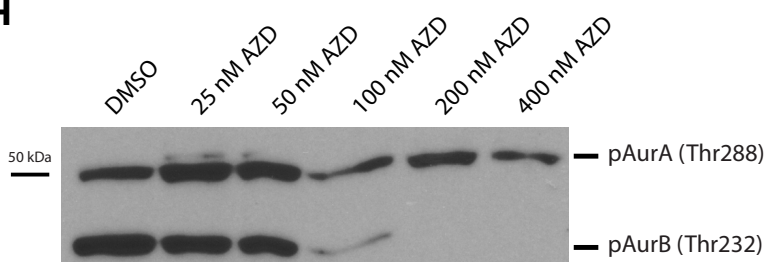
C



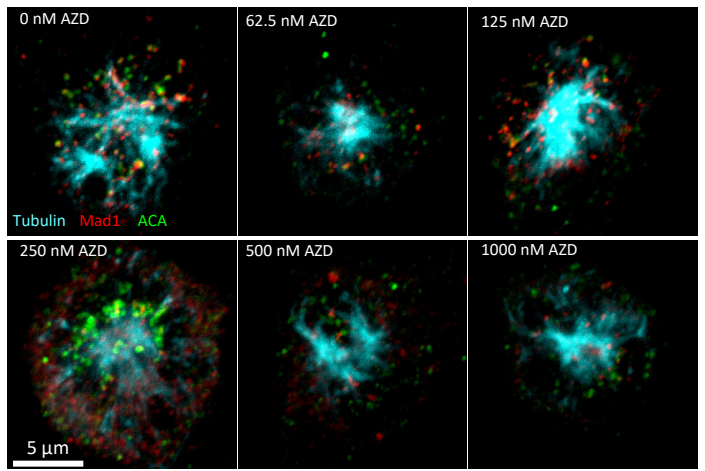
D



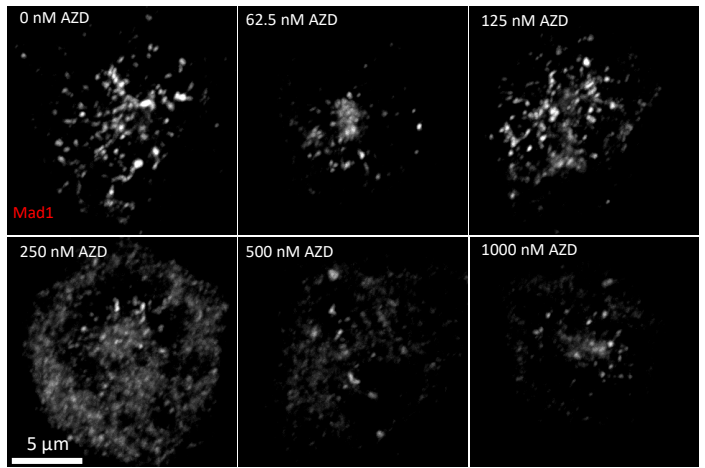
H



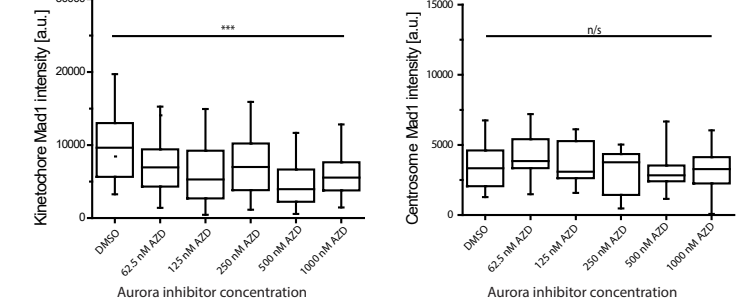
E



F



G



I

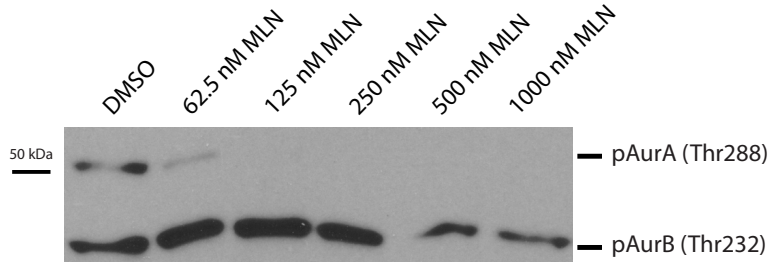
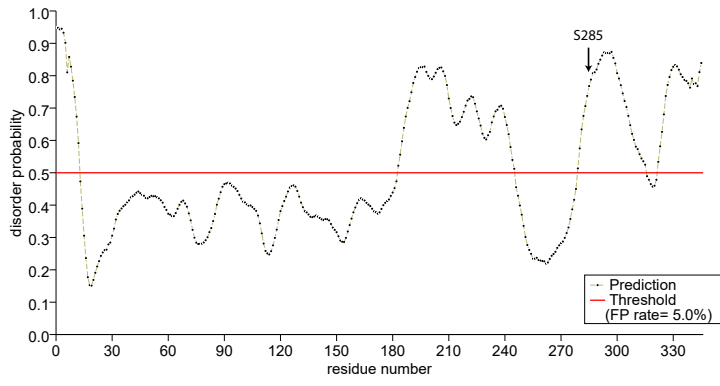
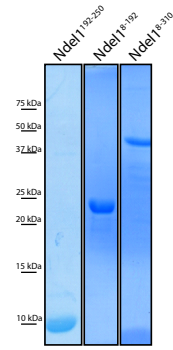


Figure S2

A



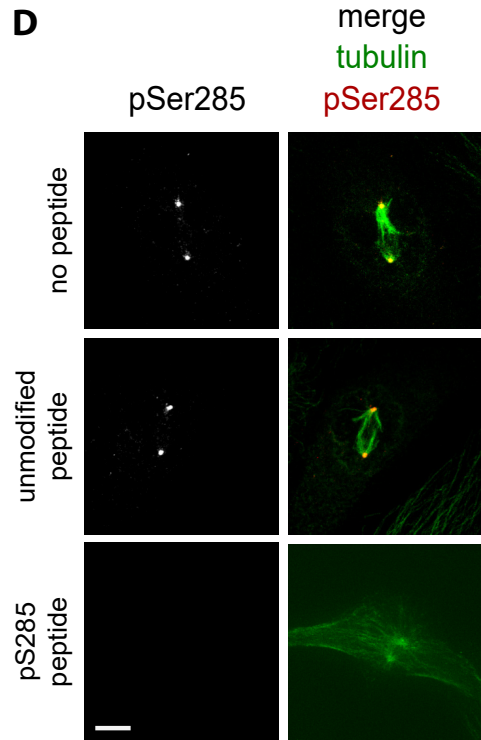
B



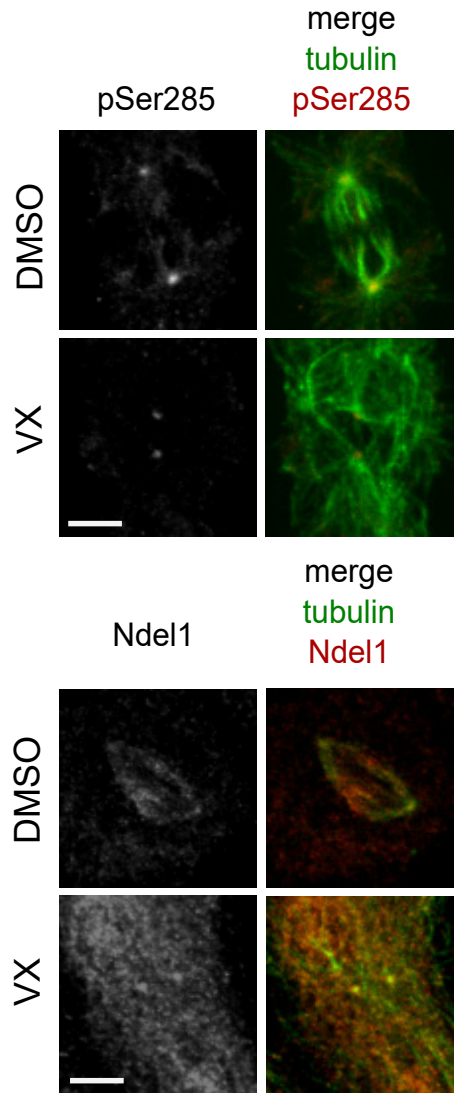
C

Phosphorylation sites	Ndel1 peptide sequence	Modification (#)
S29	KYKQ S *FQEARD	
T132	RAT I VSLDFEQRL	
T132	KRA T I ^o VSLDFEQRL	
S194	K S *APSSPTLDCEKM	
S198	KSAP S *PTLDCEKM	
T219	K.MDSAVQASLSLPAT T *PVGKG	
T219	KM#DSAVQASLSLPAT T *PVGKG	oxidation
T219	K.MDSAVQASLSLPAT T *PVGKGTENSFPSPKA	
T219	KSAPSSPTLDCEKMDSAVQASLSLPAT T *PVGKG	
S231	KG T ENSFP S *PKA	
S242	KAIPNGFG T S *PLTPSARI	
T245	KAIPNGFG T S *PLTPSARI	
S251	R I S *ALNIVGDLLRK	
S285	R K S *YVPGSVNCGVMNSNGPECP R S	
S285	R K S *YVPGSVNCGVMNSNGPECP R S	
S290	R K S *YVPG S *VNCGVMSNSNGPECP R S	
S285	R K S *YVPGSVNCGV M #NSNGPECP R S	carbamidomethyl
S194/S197/S198	K S *AP S * S *PTLDCEKMDSAVQASLSLPAT P VGKG	

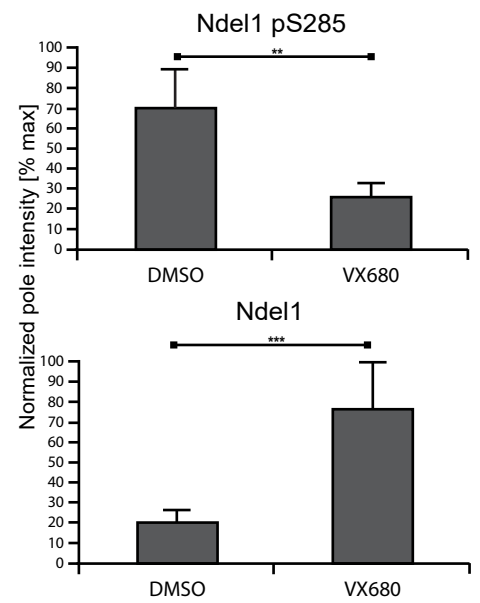
D



E



F



G

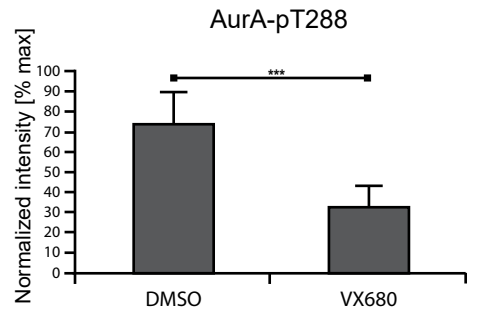


Figure S3

